

A multiple subunit Mi-2 histone deacetylase from *Xenopus laevis* cofractionates with an associated Snf2 superfamily ATPase

Paul A. Wade, Peter L. Jones, Danielle Vermaak and Alan P. Wolffe

Chromatin structure plays a crucial regulatory role in the control of gene expression. In eukaryotic nuclei, enzymatic complexes can alter this structure by both targeted covalent modification and ATP-dependent chromatin remodeling. Modification of histone amino termini by acetyltransferases and deacetylases correlates with transcriptional activation and repression [1–3], cell growth [4], and tumorigenesis [5]. Chromatin-remodeling enzymes of the Snf2 superfamily use ATP hydrolysis to restructure nucleosomes and chromatin, events which correlate with activation of transcription [6,7]. We purified a multi-subunit complex from *Xenopus laevis* eggs which contains six putative subunits including the known deacetylase subunits Rpd3 and RbAp48/p46 [8] as well as substoichiometric quantities of the deacetylase-associated protein Sin3 [9–13]. In addition, we identified one of the other components of the complex to be Mi-2, a Snf2 superfamily member previously identified as an autoantigen in the human connective tissue disease dermatomyositis [14,15]. We found that nucleosome-stimulated ATPase activity precisely copurified with both histone deacetylase activity and the deacetylase enzyme complex. This association of a histone deacetylase with a Snf2 superfamily ATPase suggests a functional link between these two disparate classes of chromatin regulators.

Address: Laboratory of Molecular Embryology, National Institute of Child Health and Human Development, National Institutes of Health, Building 18T Room 106, Bethesda, Maryland 20892, USA.

Correspondence: Alan P. Wolffe
E-mail: awlme@helix.nih.gov

Received: 15 April 1998

Revised: 7 May 1998

Accepted: 1 June 1998

Published: 22 June 1998

Current Biology 1998, 8:843–846
<http://biomednet.com/elecref/0960982200800843>

© Current Biology Ltd ISSN 0960-9822

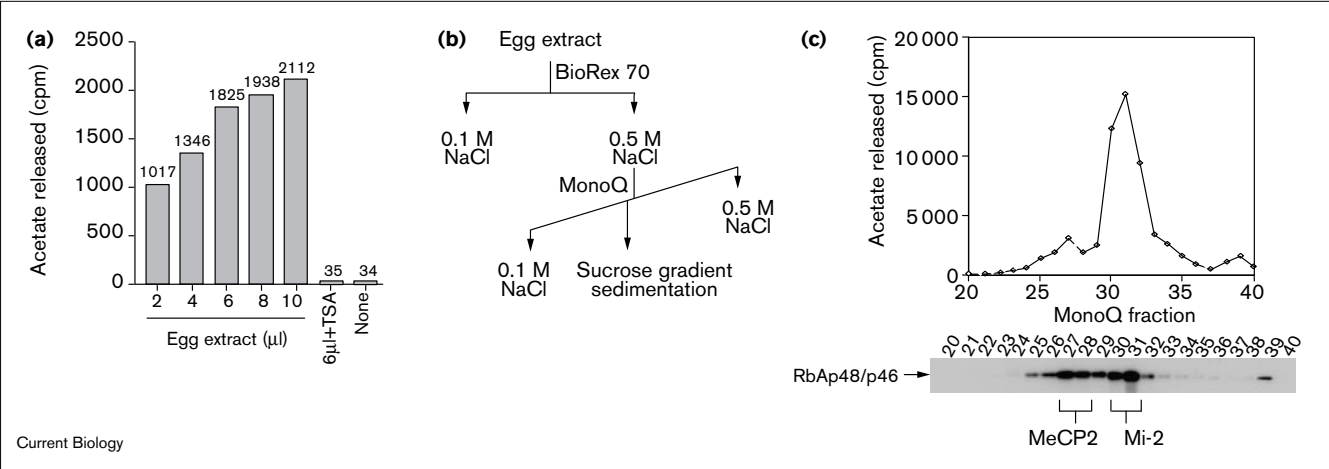
Results and discussion

Treatment of developing *Xenopus laevis* embryos with the histone deacetylase inhibitor trichostatin A perturbs normal patterns of development and gene expression [16]. This inhibitor also prevents repression mediated by the thyroid hormone receptor/9-*cis* retinoic acid receptor heterodimer (TR/RXR) in the oocyte nucleus [17], suggesting that deacetylases are present during early development

and that these enzymes perform regulatory functions in transcription. In order to understand these events at a molecular level, we have initiated a systematic biochemical analysis of histone deacetylase enzymes in *Xenopus* egg and oocyte extracts. First, we confirmed biochemically that these cells contain extractable histone deacetylase activity. Using histones acetylated by the yeast histone acetyltransferase Hat1p [18] as a substrate (see Supplementary material published with this paper on the internet), we observed robust hydrolysis of the lysine–acetate amide bond in the presence of protein from egg extracts, leading to acetate release (Figure 1a). Importantly, deacetylation was almost completely inhibited by nanomolar concentrations of trichostatin A. This demonstration of enzymatic activity in the *Xenopus* egg prompted us to characterize these enzymes further through classical fractionation and purification protocols. Although the data presented here were obtained by fractionation of egg extracts, we have obtained identical results using oocyte extracts (data not shown).

A summary of the purification protocol for one deacetylase enzyme is presented in Figure 1b (see also Table 1). This abundant enzyme was isolated through two ion exchange steps and sucrose gradient sedimentation. The initial cation exchange chromatography fractionated the extract protein into two pools eluting at 0.1 and 0.5 M NaCl, each of which contained ample deacetylase activity (data not shown). The 0.5 M NaCl elution from the BioRex column, containing approximately 15% of the total extract protein (Table 1), was further fractionated by gradient elution on MonoQ. As seen in Figure 1c, this step clearly resolved one major deacetylase activity peak from two minor ones. The first minor deacetylase peak (fraction 27) has been shown to contain the methyl CpG binding protein MeCP2 and several associated polypeptides in addition to histone deacetylase activity [19]. The major peak containing both histone deacetylase activity and RbAp48/p46 (a protein that binds to the retinoblastoma A tumor suppressor) — fractions 30 and 31 — was further purified by sedimentation on linear sucrose gradients (Figure 2a), sedimenting at a rate (by comparison to proteins of known mass) consistent with a molecular mass of 1–1.5 MDa (data not shown). Protein recovery data for this purification is reported in Table 1. Due to the presence of inhibitors and multiple enzymes with similar (or identical) activities during early stages of purification, we were unable to reliably quantitate deacetylase activity prior to the MonoQ gradient.

Figure 1



Fractionation of histone deacetylase activity from *Xenopus* egg extract. **(a)** *Xenopus* egg extracts contain histone deacetylase enzymes. Histone deacetylase activity was measured by incubating the indicated amounts of *Xenopus* egg extract with core histones acetylated *in vitro* with [3 H]acetyl coenzyme A and yeast Hat1p. Reactions proceeded for 30 min at 30°C, were terminated by acid (hydrochloric plus acetic acid), extracted with ethyl acetate, and counted in a liquid scintillation counter. Released acetate (as cpm of 3 H) is depicted in the figure. The sample in the lane marked 6 μ l + TSA contained 6 μ l extract and

trichostatin A at a final concentration of 300 nM. A reaction containing no extract was used as a control (none). **(b)** Histone deacetylase purification scheme. The flow chart summarizes the chromatographic procedures described in the text. **(c)** Cofractionation of a major deacetylase activity peak with RbAp48/p46. The indicated fractions from the MonoQ column were assayed for deacetylase activity as in (a). RbAp48/p46 was assayed by immunoblotting with an antibody against p55, the *Drosophila* homolog of RbAp48/p46. Fractions that contain the MeCP2 and Mi-2 proteins are marked beneath the blot.

The enzyme consisted of a series of cosedimenting polypeptides correlating precisely with histone deacetylase activity (Figure 2a,b). We observed major subunits of 240, 80, 66, 58, 55, and 35 kDa, with the latter four presumptive subunits migrating as doublets (or a triplet in the case of p66) in SDS-PAGE. The triplet migrating at 66 kDa stained less intensely with both Coomassie (Figure 2a and Supplementary material) and silver (see Supplementary material) staining protocols indicating that the molar ratio of the major subunits of this enzyme may not be equivalent. In addition to these predominant proteins, we observed cosedimentation of several polypeptides at clearly substoichiometric levels, particularly

proteins migrating at 190, 170, and 140 kDa (Figure 2a and Supplementary material). As Rpd3 and RbAp48/p46 homologs were known to be subunits of several recently described deacetylases [8–13], we used immunoblotting to ascertain whether these proteins were present in our enzyme preparation. We found the doublet migrating at 58 kDa to be immunoreactive using polyclonal antisera directed against *Xenopus* Rpd3 (Figure 2c). The doublet at 55 kDa was identified as RbAp48/p46 using polyclonal antisera directed against the *Drosophila* RbAp48/p46 homolog p55 (Figure 2c) and *Xenopus* RbAp48 (data not shown). Copurification of these proteins has been observed previously in other systems [8–13]. Finally, although we are able to identify a substoichiometric species at 170 kDa as the deacetylase-associated protein Sin3 using antibodies against *Xenopus* Sin3 (see Supplementary material), recovery of this polypeptide varied from preparation to preparation and we do not fully understand the nature of the interaction between Sin3 and the major subunits of this deacetylase complex.

Table 1

Protein recovery data for the purification of Mi-2.

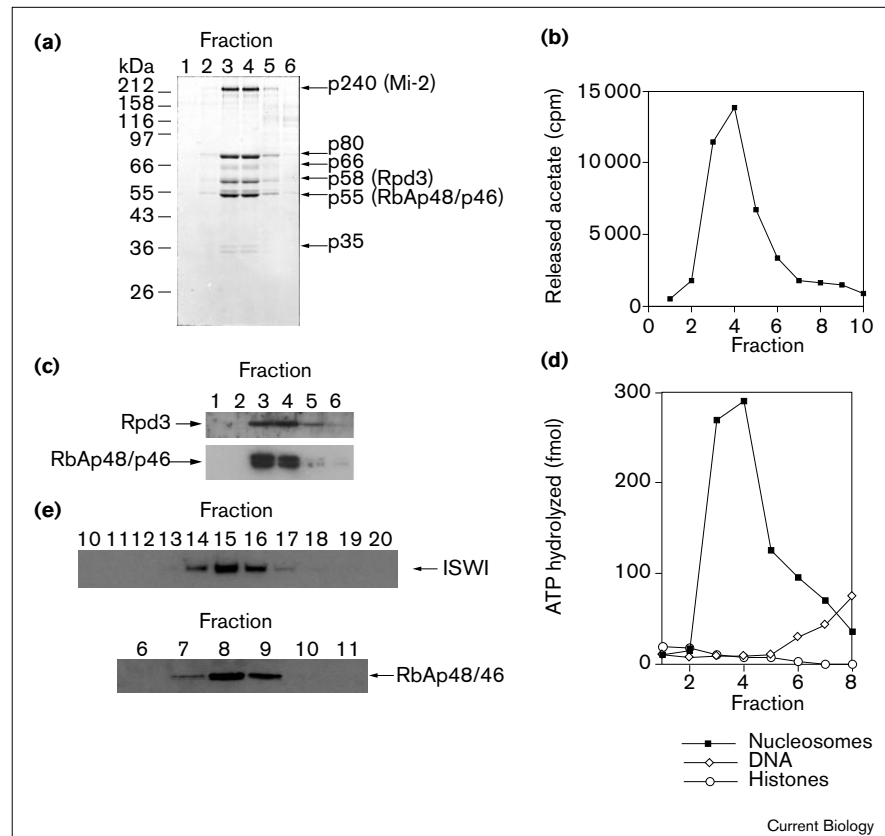
| Fraction | Volume | Protein concentration | Total protein |
|----------------|--------|-----------------------|--------------------|
| Egg extract | 136 ml | 6.9 mg/ml | 940 mg |
| BioRex 70 pool | 30 ml | 3.5 mg/ml | 105 mg |
| MonoQ 10/10 | 8 ml | 0.46 mg/ml | 3.7 mg |
| Sucrose pool | 5 ml | ≤ 0.01 mg/ml | ~ 50 μ g* |

Protein concentrations for the various fractions were determined using the BioRad protein assay following manufacturer's instructions and using bovine serum albumin as a standard. *Protein concentration estimated from Coomassie-stained gel.

We sought to identify the peptide of 240 kDa by protease digestion followed by peptide isolation, mass spectrometry and amino acid sequencing [20]. We obtained an unambiguous amino acid sequence (NIEVLGFNAR, in single-letter amino acid code) that exactly matched an amino acid sequence in Mi-2, a previously described human protein [14,15]. Mi-2 is an autoantigen in the human disease dermatomyositis and is a nuclear protein

Figure 2

A histone deacetylase complex composed of six major subunits has both deacetylase and ATPase activities. **(a,b)** Copurification of deacetylase activity with a multi-polypeptide complex. **(a)** Indicated fractions from the sucrose gradient were electrophoresed (10% SDS-PAGE) and stained with Coomassie blue. The migration of molecular weight markers is given on the left side of the gel. Arrows denote major components of the enzyme complex. **(b)** The fractions in **(a)** were assayed for deacetylase activity as described for Figure 1a. Hydrolyzed lysine-acetate amide bonds are depicted as cpm of ^3H . **(c)** Identification of RbAp48/p46 and *Xenopus* Rpd3 as subunits of the enzymatic complex. The indicated sucrose fractions were analyzed by SDS-PAGE and immunoblotting. RbAp48/p46 was detected as in Figure 1c and *Xenopus* Rpd3 was detected using anti-*Xenopus*-Rpd3 polyclonal antiserum. **(d)** Nucleosome-stimulated ATPase activity precisely cosediments with histone deacetylase activity. The sucrose gradient fractions depicted in **(a,b)** were incubated with $\gamma[^{32}\text{P}]\text{-ATP}$ and purified chicken erythrocyte mononucleosomes, salmon sperm DNA, or purified chicken erythrocyte core histones for 30 min at room temperature. Reactions were spotted on PEI cellulose thin layer chromatography plates and developed in 1 M formic acid, 0.5 M LiCl. ATP hydrolysis (in fmol) was quantitated using a phosphorimager with ImageQuant software. **(e)** *Xenopus* ISWI sediments at a vastly different rate than the Mi-2 deacetylase enzyme. The sucrose gradient fractions depicted in **(a,b)** were incubated with $\gamma[^{32}\text{P}]\text{-ATP}$ and purified chicken erythrocyte mononucleosomes, salmon sperm DNA, or purified chicken erythrocyte core histones for 30 min at room temperature. Reactions were spotted on PEI cellulose thin layer chromatography plates and developed in 1 M formic acid, 0.5 M LiCl. ATP hydrolysis (in fmol) was quantitated using a phosphorimager with ImageQuant software. **(e)** *Xenopus* ISWI sediments at a vastly different rate than the Mi-2 deacetylase enzyme. The major ISWI peak from the MonoQ gradient (Figure 1b and data not shown) was sedimented in a manner identical to the Mi-2 deacetylase. Immunoblot analysis of this gradient indicated that *Xenopus* ISWI sediments at a vastly different rate than the deacetylase enzyme (Figure 2e). Additionally, we have directly examined the Mi-2 deacetylase sucrose fractions for ISWI and failed to detect this protein (data not shown). As all other



parallel with the major deacetylase peak. Indicated sucrose gradient fractions were analyzed by SDS-PAGE and immunoblotting.

The deacetylase enzyme was detected using the anti-p55 antibody and ISWI was detected using polyclonal serum against *Xenopus* ISWI.

[14] apparently encoded by two closely related human genes also known as *HsCHD3* and *HsCHD4* [21]. Features of Mi-2 include plant homeodomain (PHD) zinc fingers, chromodomains, limited similarity to the telobox DNA-binding domain, and a Snf2 superfamily ATPase motif [14,21]. Notably, using serum from patients afflicted with dermatomyositis, Mi-2 has been observed to coprecipitate with a set of polypeptides of molecular weights that are remarkably similar to the deacetylase subunits described in this work — specifically 240, 200, 150, 72, 65, 63, 50, and 34 kDa [15]. We have confirmed the identity of the sequenced amino acids between the published human Mi-2 clones and a partial *Xenopus* cDNA clone (Genbank accession number AF059185). In addition, we obtained mass spectrometry data and partial amino acid sequence which identified a second peptide (QEESVDPDYWEK) deduced from the nucleotide sequence of the *Xenopus* cDNA clone (data not shown).

To test experimentally the possibility that *Xenopus* Mi-2 functions as an ATPase, we directly examined ATPase

activity with various cofactors. We found that ATPase activity precisely cosedimented with deacetylase activity and with the deacetylase polypeptides. Consistent with a role in modulation of chromatin structure, this activity was strongly stimulated by nucleosomes but not significantly by free DNA or histones (Figure 2d), much like the activity described for the *Drosophila* imitation switch (ISWI)-containing complex termed nucleosome remodeling factor (NURF) [22]. As Mi-2 ATPase activity had not been previously studied in the context of chromatin, we used immunoblotting to ascertain whether the nucleosome-stimulated ATPase activity we observed was in fact a property of Mi-2 or resulted from the presence of contaminating ISWI. The major ISWI peak from the MonoQ gradient (Figure 1b and data not shown) was sedimented in a manner identical to the Mi-2 deacetylase. Immunoblot analysis of this gradient indicated that *Xenopus* ISWI sediments at a vastly different rate than the deacetylase enzyme (Figure 2e). Additionally, we have directly examined the Mi-2 deacetylase sucrose fractions for ISWI and failed to detect this protein (data not shown). As all other

currently characterized chromatin ATPases are stimulated by DNA [23] — unlike the enzyme we have purified — we did not directly investigate the presence of other Swi2/Snf2 family members in the Mi-2 deacetylase sucrose fractions. We conclude that the nucleosome-stimulated ATPase activity detected in our assay is a property of Mi-2 itself and that this protein represents another member of the Snf2 superfamily of proteins which use energy from ATP hydrolysis to facilitate some aspect of chromosome metabolism [6,7,23].

The biochemical coupling of histone deacetylase and nucleosome-stimulated ATPase activities suggests that these activities may have a common functional role. The ATPase activity may be necessary to disrupt nucleosomes in order to facilitate histone deacetylation. In considering the potential biological role of this nucleosome-stimulated ATPase, we note that following fertilization, the *Xenopus* egg undergoes a series of rapid cell divisions in the absence of zygotic transcription, resulting in a 6000 cell embryo within 8 hours. These rapid mitotic cycles place an immense burden on the machinery for chromosome replication, including the machinery for histone deposition and chromatin maturation. The chromatin maturation process is known to be sequential, to involve deacetylation of the newly deposited histones (which are deposited with diacetylated histone H4, much like the substrates we have used in this study), and to result in an ordered array of nucleosomes [24]. We propose that histone deacetylase activity coupled to a nucleosome-remodeling ATPase activity is ideally suited to the process of chromatin maturation. Later in development, after the acquisition of a more 'normal' mitotic cycle, this enzyme may also perform additional functions such as the repression of individual genes or chromosomal regions following its recruitment by DNA-binding proteins or through interactions mediated by the chromodomain motif of Mi-2. Further experiments will explore these possibilities.

Supplementary material

Figures showing the histone substrates for the deacetylase assays, the quantitation of the relative amounts of the subunits of the purified deacetylase enzyme and the cosedimentation of Sin3 with Mi-2 deacetylase are published with this paper on the internet.

Acknowledgements

We gratefully acknowledge the kind gift of anti-p55 antibody from J.T. Kadonaga (UCSD) and the gift of a yeast Hat1p plasmid from M.R. Parthun (Ohio State University). We thank the members of the Laboratory of Molecular Embryology for their help and advice throughout the course of this work and Colyn Crane-Robinson for critical reading of the manuscript. Protein sequence determination was performed by the Protein/DNA Technology Center of the Rockefeller University. P.A.W. received a NRSA NIH Fellowship. P.L.J. is a PRAT fellow and D.V. is supported by a FAES/JHU graduate student stipend.

References

1. Turner BM: **Histone acetylation and control of gene expression.** *J Cell Sci* 1991, **99**:13-20.
2. Grunstein M: **Histone acetylation in chromatin and transcription.** *Nature* 1997, **389**:349-352.
3. Struhl K: **Histone acetylation and transcriptional regulatory mechanisms.** *Genes Dev* 1998, **12**:599-606.
4. Pogo BGT, Allfrey VG, Mirsky AE: **RNA synthesis and histone acetylation during the course of gene activation in lymphocytes.** *Proc Natl Acad Sci USA* 1966, **55**:805-812.
5. DePinho RA: **The cancer-chromatin connection.** *Nature* 1998, **391**:533-536.
6. Peterson CL, Tamkun JW: **The SWI/SNF complex: a chromatin remodeling machine?** *Trends Biochem Sci* 1995, **20**:143-146.
7. Tsukiyama T, Wu C: **Chromatin remodeling and transcription.** *Curr Opin Genet Dev* 1997, **7**:182-191.
8. Taunton J, Hassig CA, Schreiber SL: **A mammalian histone deacetylase related to the yeast transcriptional regulator Rpd3p.** *Science* 1996, **272**:408-411.
9. Alland L, Muhle R, Hou Jr H, Potes J, Chin L, Schreiber-Agus N, et al.: **Role for N-CoR and histone deacetylase in Sin3-mediated transcriptional repression.** *Nature* 1997, **387**:49-55.
10. Heinzel T, Lavinsky RM, Mullen T-M, Soderstrom M, Laherty CD, Torchia J, et al.: **A complex containing N-CoR, mSin3 and histone deacetylase mediates transcriptional repression.** *Nature* 1997, **387**:43-48.
11. Nagy L, Kao H-Y, Chakravarti D, Lin RJ, Hassig CA, Ayer DE, et al.: **Nuclear receptor repression mediated by a complex containing SMRT, mSin3A, and histone deacetylase.** *Cell* 1997, **89**:373-380.
12. Hassig CA, Fleischer TC, Billin AN, Schreiber SL, Ayer DE: **Histone deacetylase activity is required for full transcriptional repression by mSin3A.** *Cell* 1997, **89**:341-347.
13. Laherty CD, Yang W-M, Sun J-M, Davie JR, Seto E, Eisenman RN: **Histone deacetylases associated with the mSin3 corepressor mediate Mad transcriptional repression.** *Cell* 1997, **89**:349-356.
14. Seelig HP, Moosbrugger I, Ehrfeld H, Fink T, Renz M, Genth E: **The major dermatomyositis-specific Mi-2 autoantigen is a presumed helicase involved in transcriptional activation.** *Arth Rheum* 1995, **38**:1389-1399.
15. Nilasena DS, Trieu EP, Targoff IN: **Analysis of the Mi-2 autoantigen of dermatomyositis.** *Arth Rheum* 1995, **38**:123-128.
16. Almouzni G, Khochbin S, Dimitrov S, Wolffe AP: **Histone acetylation influences both gene expression and development of *Xenopus laevis*.** *Dev Biol* 1994, **165**:654-669.
17. Wong J, Patterson D, Imhof A, Guschin D, Shi Y-B, Wolffe AP: **Distinct requirements for chromatin assembly in transcriptional repression by thyroid hormone receptor and histone deacetylase.** *EMBO J* 1998, **17**:520-534.
18. Parthun MR, Widom J, Gottschling DE: **The major cytoplasmic histone acetyltransferase in yeast: links to chromatin replication and histone metabolism.** *Cell* 1996, **87**:85-94.
19. Jones PL, Veenstra GJC, Wade PA, Vermaak D, Kass SU, Landsberger N, et al.: **Methylated DNA and MeCP2 recruit histone deacetylase to repress transcription.** *Nature Genet* 1998, **19**:187-191.
20. Fernandez J, Andrews L, Mische SM: **An improved method for enzymatic digestion of polyvinylidene difluoride-bound proteins for internal sequence analysis.** *Anal Biochem* 1994, **214**:112-117.
21. Woodage T, Basrai MA, Baxeianis AD, Hieter P, Collins FS: **Characterization of the CHD family of proteins.** *Proc Natl Acad Sci USA* 1997, **94**:11472-11477.
22. Tsukiyama T, Wu C: **Purification and properties of an ATP-dependent nucleosome remodeling factor.** *Cell* 1995, **83**:1011-1020.
23. Wu C: **Chromatin remodeling and the control of gene expression.** *J Biol Chem* 1997, **272**:28171-28174.
24. Dimitrov S, Wolffe AP: **Chromatin and nuclear assembly: experimental approaches towards the reconstitution of transcriptionally active and silent states.** *Biochim Biophys Acta* 1995, **1260**:1-13.

A multiple subunit Mi-2 histone deacetylase from *Xenopus laevis* cofractionates with an associated Snf2 superfamily ATPase

Paul A. Wade, Peter L. Jones, Danielle Vermaak and Alan P. Wolffe

Current Biology 22 June 1998, 8:843–846

Figure S1

Histone substrates for deacetylase assays. (a) Conventional SDS–PAGE of purified chicken erythrocyte core histones before acetylation (control) and after acetylation (acetylated) with recombinant yeast Hat1p. (b) Triton acid urea gel of the same histone samples. In (a,b), the core histones are labelled at the left. In (b), the arrows on the right indicate the migration position of unacetylated (0), monoacetylated (1), and diacetylated (2) histone H4. Both Coomassie-stained gels and fluorograms of the gels are shown.

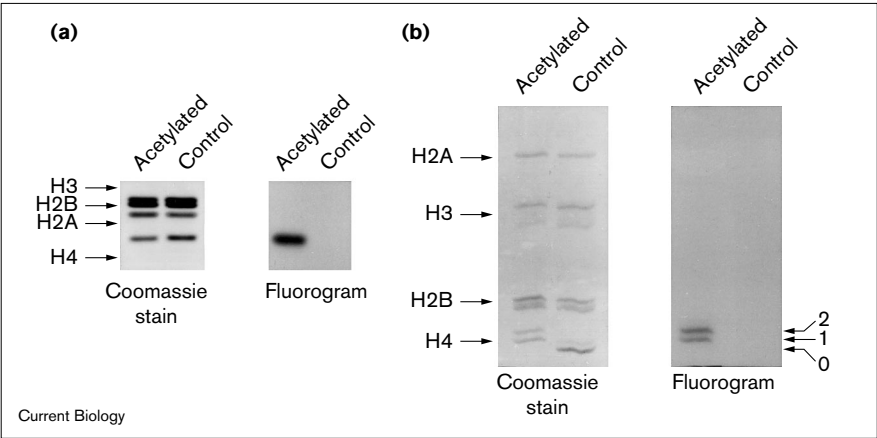
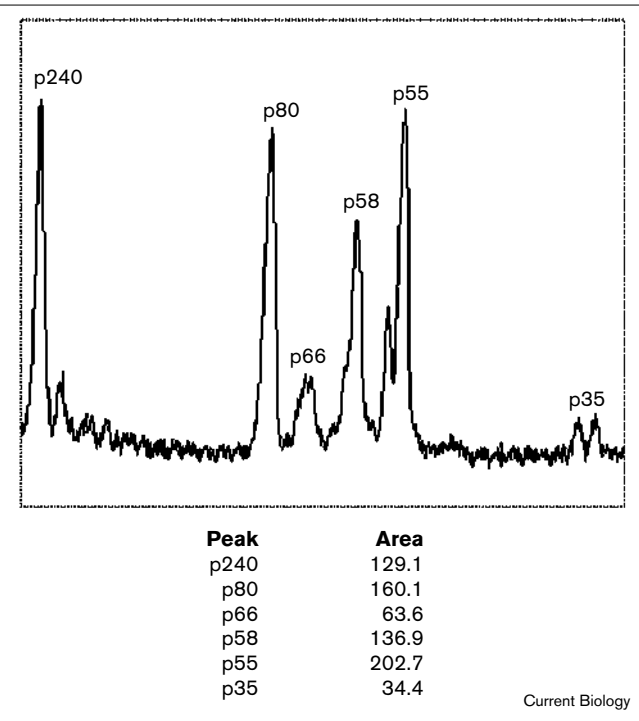
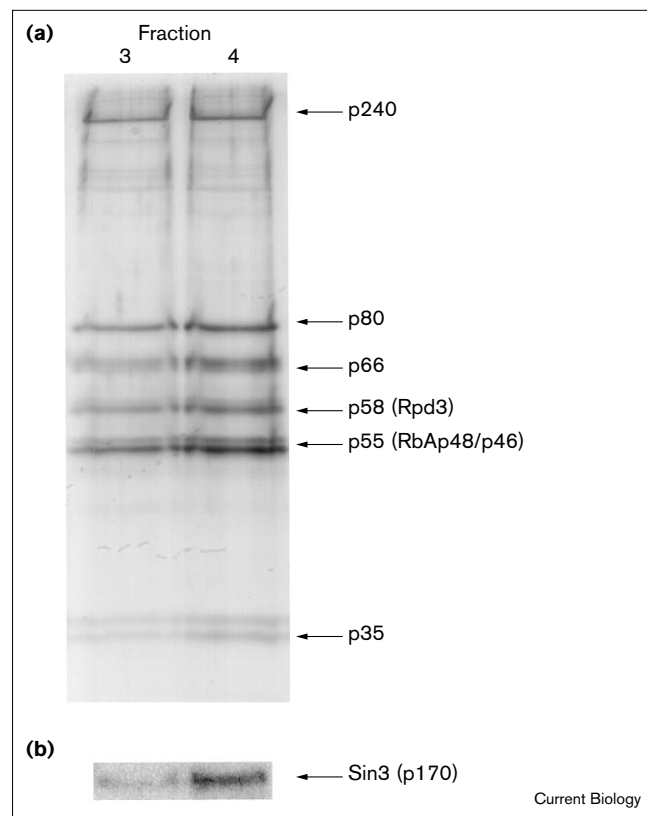


Figure S2



Densitometric scan of deacetylase enzyme. The protein gel depicted in the paper (see Figure 2a, lane 3) was scanned with a laser densitometer and the relative intensities of each band were quantitated with ImageQuant software. The areas of each peak are given in arbitrary units.

Figure S3

Coadsédimentation of Sin3 with Mi-2 deacetylase. **(a)** Sucrose fractions from the same centrifuge run depicted in Figure 2 were electrophoresed on a 10% SDS-PAGE gel and stained with silver. The peak deacetylase fractions are shown. **(b)** Sin3 immunoblot. The fractions depicted in the silver-stained gel in Figure 3a were electrophoresed, transferred to PVDF membrane and visualized with antibodies against *Xenopus* Sin3.